ORIGINAL PAPER

Shear and Rapeseed Oil Addition Affect the Crystal Polymorphic Behavior of Milk Fat

Niels Kaufmann · Jacob J. K. Kirkensgaard ·
Ulf Andersen · Lars Wiking

Abstract The effect of shear on the crystallization kinetics of anhydrous milk fat (AMF) and blends with 20 and 30 % w/w added rapeseed oil (RO) was studied. Pulse ^{1}H NMR was used to follow the α to β' polymorphic transition. The NMR method was confirmed and supported by SAXS/WAXS experiments. Samples were crystallized at 5 °C and shear of 0, 74 or 444 s^{-1} was applied during early crystallization, in the NMR tube. High shear rates decreased the amount of α polymorph formed and accelerated the polymorphic transition; however, shear did not affect the final solid fat content (SFC). The α to β' transition occurred faster in the presence of RO allowing more room for the conformational changes to occur. Final SFC decreased with increasing RO content. Shear applied in 20 and 30 % blends caused the destruction of β'-related 3L structure leaving only 2L packing. In AMF and statically crystallized samples, both 3L and 2L packing existed. Shear did not affect the amount of β crystals formed. The study shows that both shear and RO affect the polymorphic behavior of milk fat, and that ^{1}H NMR is able to detect polymorphic transition in blends with up to 30 % w/w RO.

N. Kaufmann · L. Wiking (✉)
Department of Food Science, Aarhus University,
Blichers Allé 20, P.O. Box 50, 8830 Tjele, Denmark
e-mail: Lars.wiking@agrsci.dk

J. J. K. Kirkensgaard
Niels Bohr Institute, University of Copenhagen,
2100 Copenhagen, Denmark

U. Andersen
Arla Strategic Innovation Centre, Arla Foods,
8220 Brabrand, Denmark

Introduction

Milk fat is the main constituent of butter. Butter can be blended with vegetable oil to produce a more spreadable product, and a growing market for such butter products motivates the industry to develop such new products. Milk fat is a complex fat that contains more than 400 different fatty acids in triacylglyceride (TAG) structures; 12 of these fatty acids are present in amounts above 1 % [1]. Adding a vegetable oil such as rapeseed oil (RO) will further increase the complexity of the system. The addition of vegetable oil is known to change melting behavior, microstructure, texture as well as the crystallization kinetics of anhydrous milk fat (AMF) [2, 3]. A knowledge of how processing conditions such as cooling rate, shear, and crystallization temperature affect the crystallization of milk fat blended with RO can therefore assist the dairy industry to tailor desired product properties such as mouth feel and spreadability.

Acceptable spreadability of butter or margarine depends on factors such as solid fat content, microstructure, and the polymorphic state of the TAG crystal [4]. The common polymorphic crystal forms found in milk fat are termed α, β', and β where α is a meta-stable form that re-crystallizes into the thermodynamically more stable β' form which is the predominant polymorph in milk fat [5]. The β crystals are the most stable and tend to grow large producing a grainy mouth feel which is not desirable in butter and spreads. Both β' and β modifications have been found to coexist in milk fat, however, the β polymorph is usually associated with slow crystallization that occurs at high temperatures and

long storage times [6, 7]. Mazzanti et al. [8] found that the amount of β polymorph present in the final stage of crystallization increased when more α polymorph was formed during initial crystallization and also showed that the β polymorph could form at high temperatures and at medium cooling rates. However, in general, the β polymorph is either not observed in milk fat [5, 9] or found in small amounts when a slow cooling rate are applied [4]. X-ray diffraction is the most common method used to detect, characterize, and quantify polymorphism in fats including milk fat. The polymorphic forms present in a sample can usually be deduced from diffraction patterns obtained from a small or wide-angle X-ray scattering (SAXS/WAXS) experiment. Each polymorph is characterized by specific short spacings that allows the α, β′, and β to be identified unambiguously by WAXS. Additionally, TAG crystallize in lamellar structures that span either two (2L) or three (3L) chain lengths. The long spacings usually range from 40–50 to 55–70 Å for the 2L and 3L packing, respectively, and can be determined by a SAXS experiment [6]. While α exists only as 2L packing, both β′ and β can adopt both 2L and 3L structures [10]. Differential scanning calorimetry (DSC) has also been used to detect polymorphic transformations in fat. For example, Foubert et al. [11] developed the stop-and-return technique for detecting polymorphic behavior in fats using DSC where the crystallization of the fat sample is interrupted at different times during isothermal crystallization and then melted, resulting in changes in the melting points over time which can be related to polymorphic transitions. The method is, however, time consuming. Real-time analysis of polymorphic behavior of fats during mechanical processing has been achieved by combining X-ray with a shear cell [12]. Unfortunately such equipment is not readily available. Time domain nuclear magnetic resonance (NMR) spectroscopy is routinely applied in fat research and in industry to measure solid fat content (SFC) and is widely available. Le Botlan and Ouguerram [13] proposed a method to quantify an amorphous and a solid-like phase in milk fat by analyzing the transversal relaxation decay constant from free induction decay (FID) data obtained on a low field NMR spectrometer. Since then, a number of papers using NMR to determine and characterize the polymorphic forms present in model TAG systems [14–16] and in milk fat [17] have been published. So far, NMR has been shown to successfully distinguish α and β′, however, the β modification cannot be distinguished unambiguously from β′ [14, 18]. When milk fat is cooled rapidly below 22 °C, it will initially crystallize into the meta-stable α polymorph which is characterized by carbon chain packing and dynamics that differ from that of the β′ polymorph [19, 20]. The two polymorphs produce different free induction decay curves due to the differences in molecular dynamics which form the basis for phase detection using NMR. In the present study, we monitored the polymorphic behavior of complex fat systems using a low field NMR spectrometer and applied a curve fitting method to FID data. The aim of the present study was to elucidate the effects of the addition of rapeseed oil and shear on crystal polymorphic behavior of AMF. The NMR method was supported by SAXS and WAXS experiments.

Materials and Methods

Materials

Anhydrous milk fat (AMF) was supplied by ARLA Foods (Brabrand, Denmark) and rapeseed oil (RO) was supplied by DLG FOOD Oil (Dronninglund, Denmark) and stored at −20 °C until use.

Preparation of Fat Blends

Blends of AMF with added RO (20 or 30 w/w % RO) were prepared by melting AMF at 65 °C for 30 min. The RO was added to the liquid AMF. All blends were heated to 65 °C and gently mixed just before experiments were performed.

Polymorphic Behavior Detected by Nuclear Magnetic Resonance

Standard 10-mm NMR tubes were filled with 20 ml heated fat sample and a polytetrafluoroethylene (PTFE) shear shaft with a diameter of 6 mm was inserted in each tube. The inner diameter of a tube was 9 mm leaving a 1.5-mm gap between the rod and the tube wall. Each sample was heated to 65 °C for 10 min and immediately put in a 5 °C water bath for 1 min. Then the tube was placed in the probe of the NMR and the shear shaft was mounted in the chuck of a laboratory mixer (Henry Troemner LLC, Thorofare, New Jersey). The NMR probe was an air-cooled 10-mm VT-probe (Oxford Instruments, UK) maintaining a temperature of 5 °C. The temperature was checked between each sample.

The effect of shear on the polymorphic behavior of AMF and blends was studied by applying no shear or controlled constant shear of 74 or 444 s^{-1}. Shear was applied directly in the NMR tube for the initial 10 min at 5 °C and the nominal shear rates were calculated based on the angular velocity of the shear shaft according to Eq. 1.

$$\gamma = \frac{\omega * r}{\delta} \tag{1}$$

where γ is the nominal shear rate, ω is the angular velocity of the shear shaft, r is the radius of the shear shaft (6 mm)

and δ is the gap between the tube wall and the shaft. Proton NMR free induction decay curves (FID) were recorded on a Maran Benchtop Pulsed NMR Analyzer (Resonance Instruments, Witney, UK) operating at a frequency of 23.3 MHz and equipped with a 10-mm variable temperature (VT) probe. Data was collected with P90, Dead1, Dead2 and RG set to 3.9, 4.95, 2.8, and 1 µs, respectively. FID curves were based on 8 scans. A script was created using the software supplied with the NMR to collect a FID curve every 1.5 min. During NMR data acquisition, shear was switched off. In addition, a set of FID curves were measured on an empty tube including a shear shaft. This FID was subtracted from the sample FID to eliminate noise caused by the tube and shear shaft. The FID curves were fitted with Eq. 2 using the R statistical computing software and the NLS (nonlinear least-squares) function (R Foundation for Statistical Computing, Vienna, Austria) to determine the least-squares estimates of the parameters in the equation.

$$F(t) = A \times \exp\left(\frac{-t^2}{\tau^2}\right) + B \times t + C \qquad (2)$$

$F(t)$ is the collected FID data, t is the time and τ is the solid-state decay constant and A, B, and C are fitted parameters.

Solid Fat Content Determination of Blends

Solid fat content was calculated from the FID curves using the direct method according to the official AOCS method (AOCS, cd16b-93). The method relies on a predetermined F- and k-factor calculated from FID curves collected on calibration standards. The calibration factors were obtained from the SF direct software supplied with the 10-mm probe.

X-ray Analysis of Blends

Combined small- and wide-angle X-ray scattering (SAXS/WAXS) was performed using the SAXSLab instrument (JJ-Xray, Denmark) equipped with a 100XL + microfocus sealed X-ray tube (Rigaku, The Woodlands Texas) and a 2D 300 K Pilatus detector (Dectris Ltd., Baden, Switzerland). Measurements were performed with a pin-hole collimated beam with the detector positioned asymmetrically to yield a single measurement q-range of 0.05–2.8 Å^{-1}. Here the magnitude of the scattering vector is defined as $q = 4\pi\lambda/\sin(\theta)$, with $\lambda = 1.54$ Å^{-1} being the X-ray wavelength and θ half of the scattering angle. In this setting all relevant peak information for both short and long spacings can be obtained in a single measurement [21]. The samples were sealed between two 5–7 µm thick mica windows and measurements were performed in vacuo. The non-sheared samples were loaded onto a temperature controlled sample stage (Linkam Scientific Instruments Ltd., Tadworth, UK) and were cooled from 60 to 5 °C at 10 °C/min before measuring started. In shear experiments, shear was applied in NMR-tubes as described previously. Immediately after the shear step was ended, samples were transferred to pre-cooled sample holders and then measured. Due to the time delay associated with this sample transfer, sheared samples had basically lost any shear-induced orientation of the crystalline structure. In a few cases very faint indications of orientation are apparent but made no detectable difference in the averaged spectra (tested, not shown). All measurements were 60 s long. The data were radially averaged using standard reduction procedures.

Statistical Analyses

The effect of RO content and shear rate was analyzed using the PROC GLM procedure (SAS Institute, Cary, NC, USA). $P < 0.05$ was used as the significance threshold.

Results and Discussion

Detecting Crystal Polymorphic Transition in AMF by Using Pulsed NMR

We obtained FID curves of AMF after 10 and 60 min of isothermal crystallization at 5 °C (Fig. 1) and the data were fitted by an ensemble of Gaussian and linear functions (Eq. 2). The curve fitting method produced a solid state decay constant (τ) [22]. As the carbon chain packing of the TAG changed as a result of less dense α crystals transforming into β' crystals, the fitted parameter τ decreased. The FID curves obtained after 10 and 60 min were fitted giving τ values of 22.8 and 15.5 µs, respectively. Combined SAXS and WAXS spectra of AMF isothermal crystallization over 1 h showed that after 10 min only the α polymorph was present, while after 60 min peaks corresponding to α, β' and β had appeared (Fig. 2). The decrease in τ corresponded with the transition observed in the SAXS/WAXD experiment. After 60 min, a mix of β' and detectable amounts of α and β were present (Fig. 2b), so it was not possible to relate the τ of 15.5 µs reported after 60 min to β' alone.

The residuals between the FID measurements and the theoretical curve (Fig. 1b, d) appeared normally distributed around zero, which demonstrated a good fit. After 60 min of isothermal crystallization (Fig. 1c) a faint irregularity was observed around 30–60 µs. The residuals plot (Fig. 1d) showed that Eq. 2 cannot accurately describe this part of the FID data. Previous studies of polymorphism in

fat by NMR reported that the presence of both β' and β polymorphs are commonly accompanied by such irregular FID patterns, termed a beat pattern, which were observed around 20–60 µs [14, 18]. These irregularities were caused by dipolar interactions between neighboring protons [23]. A faint beat pattern first appeared after 25 min of isothermal crystallization, indicating the presence of β'/β polymorph. The first traces of β' in AMF were observed in WAXS after 21–23 min (Fig. 2). The beat pattern caused the residual sum of squares (RSS) to increase, however, the residuals obtained on samples after 60 min still suggested a reasonable fit and allowed the α polymorph to be distinguished from β'.

The values of the solid state decay reported in the present study are generally higher than those reported in the study by Janssen et al. [22] where AMF was crystallized at 10, 15, and 22 °C. It is likely that the higher crystallization temperature used in their study resulted in formation of less of the α polymorph which explains the overall lower τ that was reported. To determine if τ would decrease further, we analyzed a sample after 24 h and τ

decreased to 13.5 µs (data not shown), suggesting that small amounts of α polymorph can exist for a long time in AMF.

Thus, the solid state decay data obtained by using the NMR method successfully detected the polymorphic behavior of statically crystallized AMF and the results could be correlated to WAXS data.

## Effect of Rapeseed Oil on Polymorphic Behavior

Figure 3 shows the crystal polymorphic behavior for AMF and blends with 20 and 30 % w/w RO in the absence of shear which were quenched by cooling to 5 °C. In general, the behavior was the same for all fats although the peaks are most pronounced in pure AMF. Only α was present after 5 min and this form gradually transformed into β' and traces of β. Hence, after 60 min of isothermal crystallization, β' dominated with traces of α and β. The SAXS data revealed that addition of RO increased the lamellar spacing from 73.8 Å for AMF to 74.6 and 75.6 Å for 20 and 30 % w/w, respectively (Fig. 3).

Fig. 1 Free induction decay curves measured in AMF after 10 (**a**) and 60 (**c**) min of isothermal crystallization at 5 °C. The data was fitted by a combination of gaussian and linear functions (*dashed line*). Residuals of the fit after 10 (**b**) and 60 min (**d**)
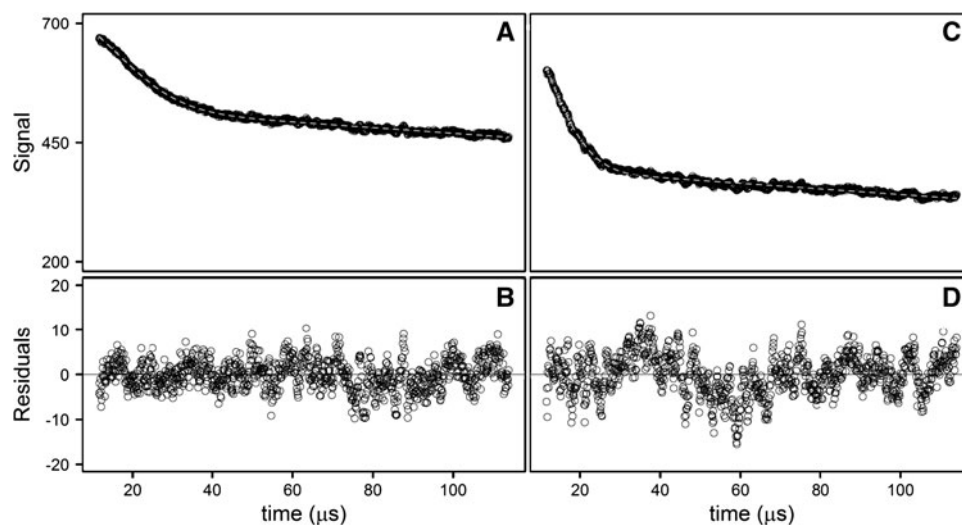
Fig. 2 Combined SAXS and WAXS spectra of AMF analyzed at 10 (**a**) and 60 min (**b**) after quenching to 5 °C. WAXS diffraction peaks corresponding to α, β', and β are indicated
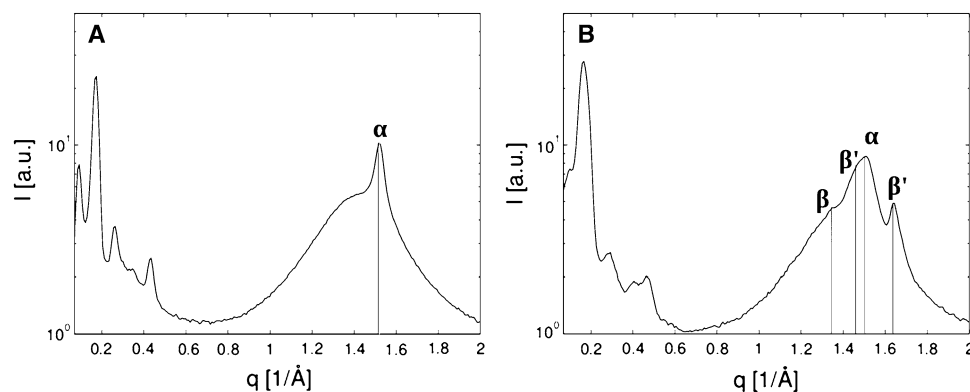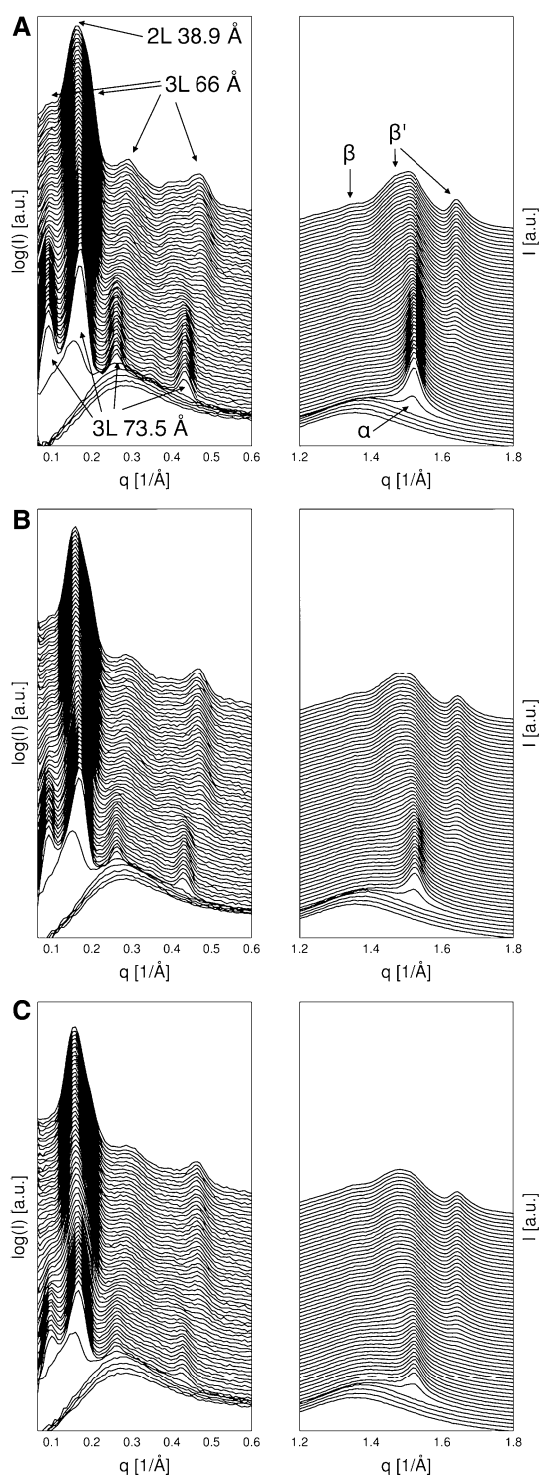
Fig. 3 SAXS (left) and WAXS (right) spectra from quenched samples containing AMF (**a**), 20 % (**b**), and 30 % (**c**) RO. The first curve is shown at the bottom of each graph and all other curves were recorded at intervals of 1 min 16 s. The peak assignments used in (**a**) sample apply to all three plots

The effect of RO addition on the polymorphic behavior of AMF was also studied by NMR. The τ from crystallizing AMF and the 20 and 30 % blends without shear were plotted as a function of isothermal crystallization time (Fig. 4a). A FID curve was collected every 1.5 min during isothermal crystallization. Each point in Fig. 4 corresponds to a τ value obtained from one FID curve. When crystallizing AMF at 5 °C without shear, a maximum τ of 23.5 µs was reached after 5 min of isothermal crystallization corresponding to the presence of the α polymorph only, as observed in Fig. 3a. Under static conditions, maximum τ was unaffected by adding 20 % RO, however, addition of 30 % RO decreased ($P < 0.05$) the maximum τ from 23.5 in AMF to 22.0 µs. WAXS analysis for the 30 % blend detected only the diffraction peak from the α polymorph in the initial crystallization phase (Fig. 3c), thus the decrease in τ (Fig. 4a) is presumably not related to the formation of the β' polymorph. It was not possible to fully explain the observed decrease in τ, although RO is known to solubilize part of the AMF TAG and thereby changes the composition of AMF crystals [24, 25]. Herrera and Hartel speculated that partial solubilization of TAG containing short chain or unsaturated fatty acids could result in denser packing [30], an event which could decrease crystal long spacing. While this could cause a decrease in τ, this was not observed in our study. In contrast, addition of RO caused swelling of the lamella α crystal packing, resulting in a small increase of long spacings as the RO content increased (Fig. 3). WAXS data in Fig. 3 clearly shows the liquid phase, whereas the NMR data (Fig. 4.) only provides information about the crystalline phase.

The NMR method revealed that during the isothermal crystallization, increased RO content slightly decreased the onset time of the α to β' transition. In blends with 20 or 30 % RO, the transition occurred at 14 and 11 min, respectively, and at 15 min in AMF (Fig. 4a). This observation was further supported by SAXS/WAXS data (Fig. 5) which showed the relative peak intensity of the most abundant polymorphic forms during static crystallization of AMF and blends. (The vertical dashed lines in Fig. 5 are correlated with important structural events). In all samples, α crystals first appeared after 5–6 min of isothermal crystallization. The α to β' transition started at 21, 18, and 16 min in AMF, the 20 % and the 30 % blends, respectively. The close proximity of some peaks gave the potential risk of one peak artificially increasing another.
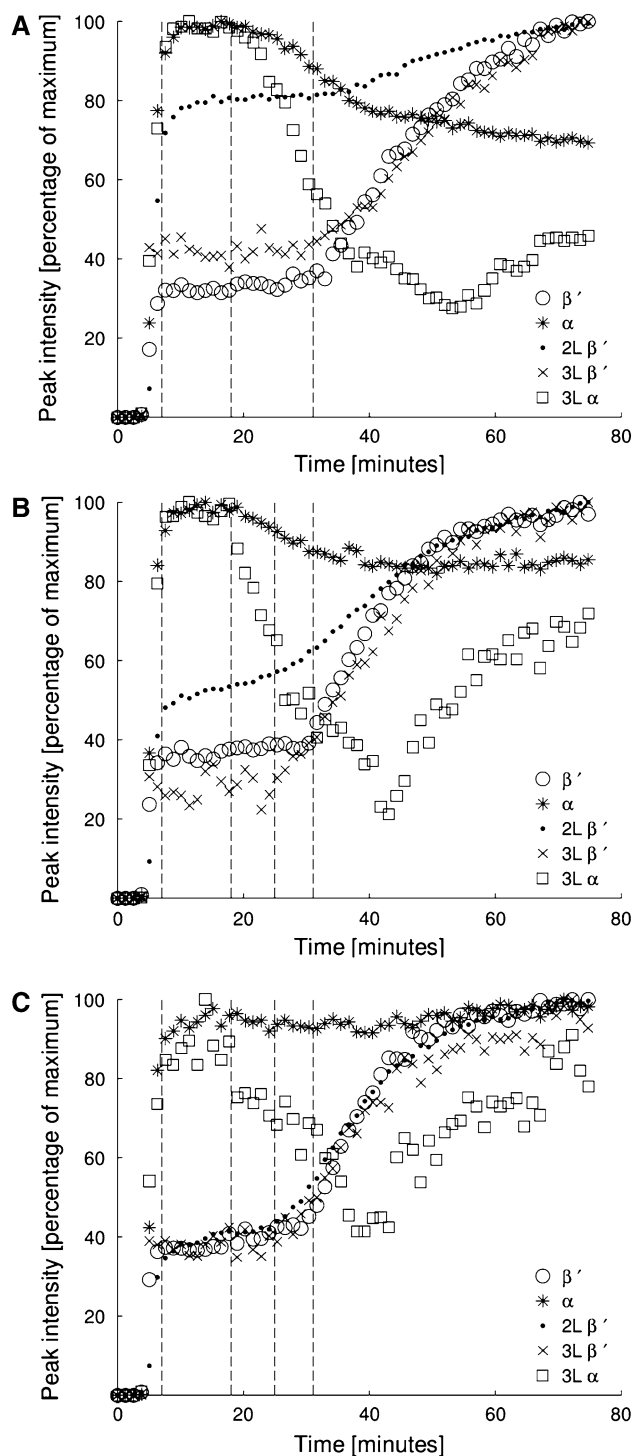
NMR and SAXS/WAXS methods showed similar α to β' transition patterns, however, the onset of the transition occurred later in the SAXS/WAXS experiments. This difference is attributed to the fact that cooling profiles used in the two methods were not exactly the same. In the latter method, samples were cooled to 5 °C at a constant rate of 10 °C/min made possible by the low sample size. This rate was chosen because it was found to be the average cooling rate when a fat sample was quenched by cooling directly in a 5 °C water bath. However, in practice, cooling is initially
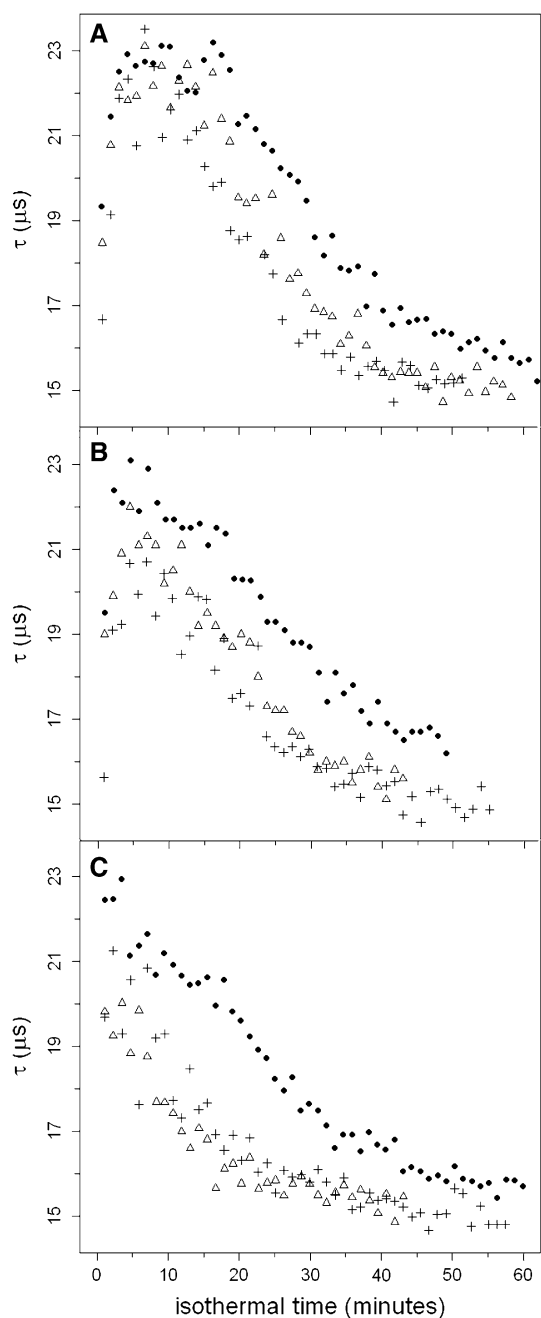
Fig. 4 Fitted solid state relaxation constant (τ) plotted as a function of isothermal crystallization time for AMF (*filled circles*), 20 % (w/w) RO (*triangles*) and 30 % (w/w) RO (*plus signs*). No shear (**a**) or shear rates of 74 s^{-1} (**b**) or 444 s^{-1} (**b**) was applied during the initial 10 min of crystallization at 5 °C

Fig. 5 Peak intensity of the most abundant crystals forms in quenched cooled AMF (**a**) and blends with 20 % (**b**) and 30 % (**c**) RO. *Vertical dashed lines* at 7, 18, 25 (blends only) and 31 min are included to emphasize important structural events

faster and slows as the temperature decreases toward the bath temperature of 5 °C.

The earlier polymorphic transition observed when the liquid fraction is increased could be caused by more space in the crystal network which favors the considerable conformational changes related to α to β' transition. For example, the re-crystallization from β' to β of the high

melting fraction of milk fat only occurs in the presence of liquid oil [26]. Also an earlier onset of transition could occur in blends due to the decreased concentration of AMF TAG from RO dilution. Lower super-saturation of TAG

would decrease the driving force toward crystallization and thus less α polymorph would be formed.

The SAXS experiment revealed an interesting property of AMF crystallization in the presence of RO. In Fig. 5, the β′ long spacings appear before the short spacings indicating that the lamellar ordering precedes the actual packing into the transverse crystalline form. This was observed both in 20 and 30 % blends although with slightly different progressions. In the 20 % blend, the long spacing had already formed after 15 min while in the 30 % blend it occurred after 20 min. We concluded that the increased liquid fraction allowed the TAG to adopt the lamellar structure more readily and this pre-ordering likely accelerated β′ formation. The early transition of α to β′ in the presence of RO compared to pure AMF could be attributed to the factors discussed earlier. Another possible interpretation may be that the SAXS peaks are stronger and easily observed earlier than the WAXS peaks. This does, however, not explain why no WAXS peaks are observed before SAXS peaks in pure AMF.
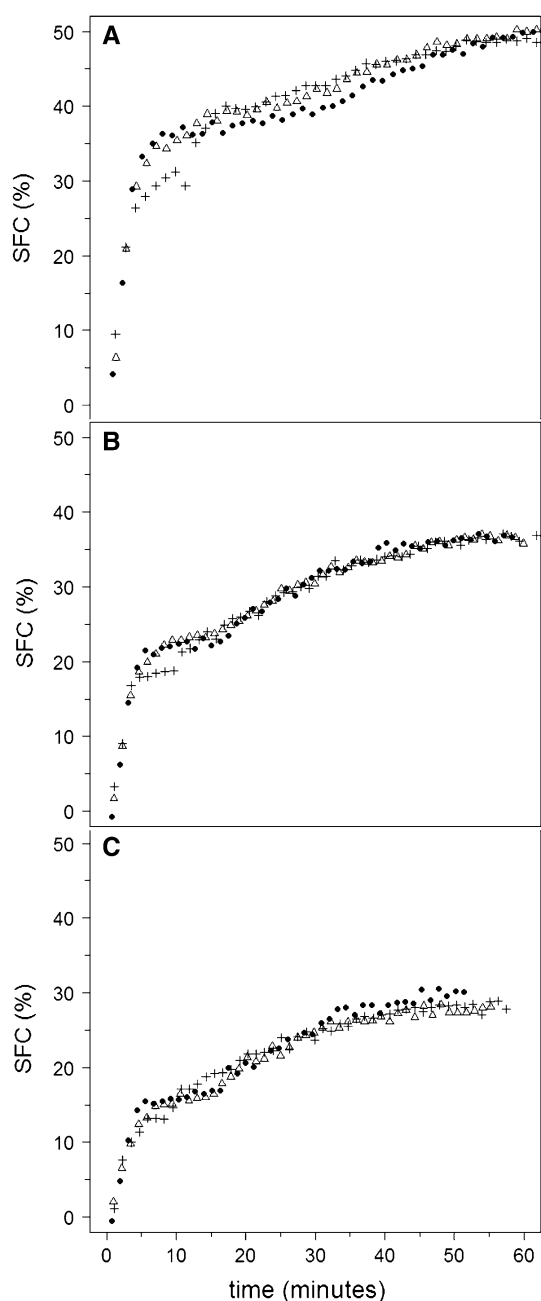
Effect of Shear on the Polymorphic Behavior

The application of high shear forces [74 s^{-1} (Fig. 4b) and 444 s^{-1} (Fig. 4c)] to AMF significantly ($P < 0.005$) decreased τ from 23.0 to 20.8 μs after 5 min of isothermal crystallization as compared to statically crystallized AMF (Fig. 4). Also in blends with 20 or 30 % RO, the value of τ was significantly ($P < 0.05$) lower at high shear compared to no shear after 5, 10, 15, and 20 min. Thus, high shear accelerated the α to β′ transition in 20 and 30 % RO blends as well as in AMF. In previous studies with AMF crystallized at 17.5 °C it was found that increasing the shear rate accelerated the crystallization and, subsequently, an earlier transition from α to β′ crystals, even at a low shear rate of 45 s^{-1} [8, 12]. In the present study, the intermediate shear rate of 74 s^{-1} tended to accelerate the transition development for AMF compared to static conditions ($P < 0.1$). Samples crystallized with shear of 444 s^{-1} were also analyzed by SAXS/WAXS, however, due to the need for transferring the sheared samples into the sample cells, the earliest data point corresponds to 20 min of isothermal crystallization. Figure 6 display the quenched and sheared samples after 20, 30, and 40 min of crystallization. From the WAXS spectra it is clear that shearing accelerates polymorphic transition from α to β′. For example, the spectrum for non-sheared AMF shows only one peak after 20 min, corresponding to α, whereas for the sheared sample two diffraction peaks co-existed, corresponding to β′ which was also observed along with α (Fig 6a). In blends crystallized with high shear, β′ seemed to dominate over the α form after 20 min suggesting that RO complements the effect of shear by further accelerating the transition.
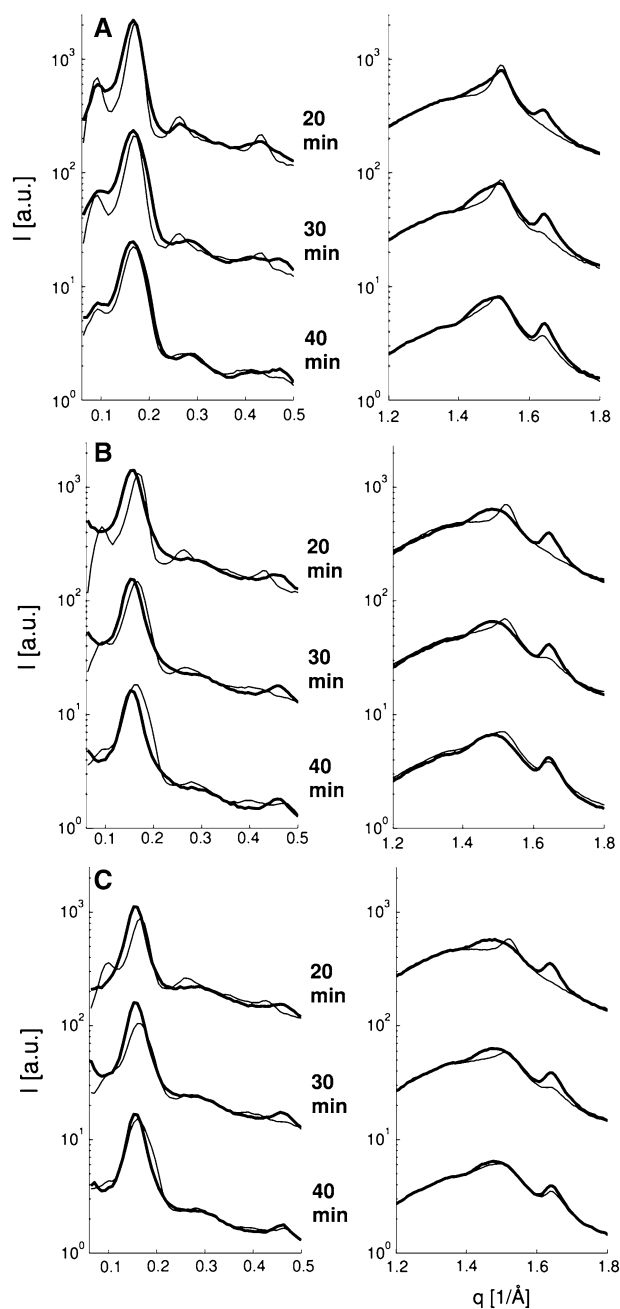
Fig. 6 SAXS (*left*) and WAXS (*right*) spectra of AMF (**a**) and blends with 20 % (**b**) and 30 % (**c**) RO statically crystallized (*thin lines*) or crystallized under shear (444 s^{-1}) (*thick lines*). The passage of time from quench cooling to 5 °C is indicated in the figure

Even after 40 min of crystallization sheared samples were richer in β′ crystals compared to non-sheared samples. After 30 and 40 min all samples had an indication of an additional peak at 4.6 Å caused by small amounts of the β polymorph. No effect of shear on β formation was observed.

Shear affected the long spacings (Figs. 6b and 5c). Without shear, both 2L and 3L packing were present,

Fig. 7 SFC plotted as a function of isothermal crystallization time for AMF (**a**), 20 % (w/w) RO (**b**), and 30 % (w/w) RO (**c**). No shear (*filled circles*) or shear rates of 74 s^{-1} (*triangles*) or 444 s^{-1} (*plus signs*) was applied during the initial 10 min of crystallization

TAG chain lengths [15], while longitudinal relaxation has been shown to vary with crystal size [28]. In the present paper, the transversal relaxation decay was studied, hence a great effect on the decay data from decreasing crystal size due to shear is not expected. However, blending AMF with RO could potentially change the TAG composition in the crystals and cause changes in the average TAG chain length in the crystallized fat. Blending AMF with RO caused a slight change in TAG composition of AMF crystals [3], however the small changes observed are not likely to change the relaxation properties being studied here.

Solid Fat Content of AMF and Blends Crystallized Under Shear Flow

The SFC was calculated from FID data. In Fig. 7, the SFC of AMF and blends is plotted as a function of isothermal crystallization time. As expected, SFC decreased with increasing amounts of RO in 20 and 30 % RO blends. All samples showed the characteristic two step crystallization, where SFC increased and reached a plateau followed by a second SFC increase, as previously observed in AMF related to α to β′ transition [29]. The major part of the solids crystallized within the first 10 min of crystallization due to fast crystallization kinetics at 5 °C. In general, the final SFC was not affected by shear. This result is in agreement with previous studies of milk fat and cacao butter crystallized under shear [30, 31]. The development of SFC was, however, affected. When a shear rate of 444 s^{-1} was applied, the first crystallization step reached a plateau at a lower SFC compared to no shear. Shortly after shear was halted, SFC increased rapidly to the same level as samples crystallized without shear or at a shear rate of 74 s^{-1}. Mudge et al. [31] applied a continuous shear and found that high shear rates led to lower SFC values compared to low shear. In this case a constant high shear seemed to continuously prevent the growth of crystals. All together this suggests that high shear breaks the growing crystals and thereby prevents or delays further crystallization.

Conclusion

In this study pulsed NMR was used to detect polymorphic behavior of AMF and oil blends crystallized under shear by applying a curve fitting method to FID data and monitoring transversal decay characteristics of samples as a function of crystallization time. It was possible to follow the transition from the α to the β′ polymorph, both in statically crystallized and in sheared samples. In general, the polymorphic behavior observed by NMR was in good agreement with

however, high shearing of blends destroyed the 3L packing leaving a pure 2L arrangement with a length of 38.9 Å. In AMF, the 3L packing was not destroyed by shear.

It is known that shear decreases the crystal cluster size of a crystallized fat [17, 27]. The effect of the crystal cluster size on the solid state decay constant was not examined. A previous study had shown that the transversal relaxation decay of pure TAG is affected by changes to

SAXS/WAXS data. The α to β′ transition was accelerated by increased shear rate. Furthermore, addition of RO also resulted in earlier transition to β′ form. This more rapid transition time was ascribed to higher mobility due to the increased liquid fraction. Addition of RO also caused lamellar ordering prior to actual transverse crystallization. High shearing destroyed the 3L packing in blends with 20 and 30 % RO but not in pure AMF. NMR provided information about the polymorphic behavior from the start of crystallization and throughout crystallization, while X-ray provided more detailed information about the crystal packing such as swelling of the crystals in blends. However, NMR offered the advantage of allowing us to study the early phase of crystallization of samples under shear. In general, the NMR method used in this study performed well and predicted the phase behavior of the samples studied. This study shows that this method can potentially be applied to study the effects of shear on polymorphism in other complex lipid systems.

References

1. Jensen RG (2002) The composition of bovine milk lipids: January 1995 to December 2000. J Dairy Sci 85:295–350
2. Kaufmann N, Andersen U, Wiking L (2012) The effect of cooling rate and rapeseed oil addition on the melting behaviour, texture and microstructure of anhydrous milk fat. Int Dairy J 2:73–79
3. Wright AJ, Batte HD, Marangoni AG (2005) Effects of canola oil dilution on anhydrous milk fat crystallization and fractionation behavior. J Dairy Sci 88:1955–1965
4. Campos R, Narine SS, Marangoni AG (2002) Effect of cooling rate on the structure and mechanical properties of milk fat and lard. Food Reson Int 35:971–981
5. Ten Grotenhuis E, Van Aken G, van Malssen K, Schenk H (1999) Polymorphism of milk fat studied by differential scanning calorimetry and real-time X-ray powder diffraction. J Am Oil Chem Soc 76:1031–1039
6. Lopez C (2002) Crystalline structures formed in cream and anhydrous milk fat at 4 °C. Le Lait 82:317
7. Lopez C, Bourgaux C, Lesieur P, Bernadou S, Keller G, Ollivon M (2002) Thermal and structural behavior of milk fat. 3. influence of cooling rate and droplet size on cream crystallization. J Colloid Interface Sci 254:64–78
8. Mazzanti G, Guthrie SE, Sirota EB, Marangoni AG, Idziak SHJ (2004) Effect of minor components and temperature profiles on polymorphism in milk fat. Cryst Growth Des 4:1303–1309
9. Fredrick E, Van de Walle D, Walstra P, Zijtveld JH, Fischer S, Van der Meeren P, Dewettinck K (2011) Isothermal crystallization behaviour of milk fat in bulk and emulsified state. Int Dairy J 21:685–695
10. Himawan C, Starov VM, Stapley AGF (2006) Thermodynamic and kinetic aspects of fat crystallization. Adv in Colloid Interface Sci 122:3–33
11. Foubert I, Fredrick E, Vereecken J, Sichien M, Dewettinck K (2008) Stop-and-return DSC method to study fat crystallization. Thermochim Acta 471:7–13
12. Mazzanti G, Marangoni AG, Idziak SHJ (2009) Synchrotron study on crystallization kinetics of milk fat under shear flow. Food Reson Int 42:682–694
13. Botlan DJ, Ouguerram L (1997) Spin–spin relaxation time determination of intermediate states in heterogeneous products from free induction decay NMR signals. Anal Chim Acta 349:339–347
14. Trezza E, Haiduc AM, Goudappel GJW, van Duynhoven J (2006) Rapid phase-compositional assessment of lipid-based food products by time domain NMR. Magn Reson Chem 44:1023–1030
15. Berret MA, Riaublanc AM, Mouro CR, Mariette F (2008) Study of triacylglycerol polymorphs by nuclear magnetic resonance: effects of temperature and chain length on relaxation parameters. Magn Reson Chem 46:550–557
16. Berret MA, Riaublanc AM, Mariette F (2009) Effects of crystal growth and polymorphism of triacylglycerols on NMR relaxation parameters. 2. Study of a tricaprin–tristearin mixture. Cryst Growth Des 9:4281–4288
17. Maleky F, Marangoni A (2011) Thermal and mechanical properties of cocoa butter crystallized under an external laminar shear field. Cryst Growth Des 11:2429–2437
18. Duynhoven J, Dubourg I, Goudappel GJ, Roijers E (2002) Determination of MG and TG phase composition by time-domain NMR. J Am Oil Chem Soc 79:383–388
19. Painter KL, Williams SD, Hartel RW (1997) Incorporation of milk fat and milk fat fractions into compound coatings made from palm kernel oil. J Dairy Sci 80:2237–2248
20. Marangoni AG, Lencki RW (1998) Ternary phase behavior of milk fat fractions. J Agric Food Chem 46:3879–3884
21. Rønholt S, Kirkensgaard J, Pedersen TB, Mortensen K, Knudsen JC (2012) Polymorphism, microstructure, and rheology of butter. Effects of cream heat treatment. Food Chem. doi:10.1016/j.foodchem.2012.05.087
22. Janssen P, MacGibbon A (2007) Non-isothermal crystallization of bovine milk fat. J Am Oil Chem Soc 84:871–875
23. Derbyshire W, van den Bosch M, van Dusschoten D, MacNaughtan W, Farhat IA, Hemminga MA, Mitchell JR (2004) Fitting of the beat pattern observed in NMR free-induction decay signals of concentrated carbohydrate water solutions. J Magn Res 168:278–283
24. Wright AJ, Batte HD, Marangoni AG (2005) Effects of canola oil dilution on anhydrous milk fat crystallization and fractionation behavior. J Dairy Sci 88:1955–1965
25. Kaufmann N, Andersen U, Wiking L (2012) The effect of cooling rate and rapeseed oil addition on the melting behaviour, texture and microstructure of anhydrous milk fat. Int Dairy J 2:73–79
26. Timms RE (1980) The phase behaviour and polymorphism of milk fat, milk fat fractions and fully hardened milk fat. Aust J Dairy Technol 35:47–53
27. de Graef V, van Puyvelde P, Goderis B, Dewettinck K (2009) Influence of shear flow on polymorphic behavior and microstructural development during palm oil crystallization. Eur J Lipid Sci Technol 111:290–302
28. Berret MA, Riaublanc AM, Mouro CR, Mariette F (2009) Effects of crystal growth and polymorphism of triacylglycerols on NMR relaxation parameters. 1. Evidence of a relationship between crystal size and Spin–Lattice relaxation time. Cryst Growth Des 9:4273–4280
29. Cisneros A, Mazzanti G, Campos R, Marangoni AG (2006) Polymorphic transformation in mixtures of high- and low-melting fractions of milk fat. J Agric Food Chem 54:6030–6033

30. Herrera ML, Hartel RW (2000) Effect of processing conditions on physical properties of a milk fat model system: Rheology. J Am Oil Chem Soc 77:1189–1195

31. Mudge EM, Mazzanti G (2009) Rheo-NMR measurements of cocoa butter crystallized under shear flow. Cryst Growth Des 9:3111–3118